

Stability of fluid layers carrying a normal electric current

By A. D. SNEYD

University of Waikato, Hamilton, New Zealand

(Received 20 June 1984 and in revised form 5 December 1984)

This paper attempts to explain MHD instabilities observed in aluminium reduction cells. The model analysed is a plane horizontal poorly conducting fluid layer, sandwiched between two highly conducting semi-infinite layers, the lower one a fluid and the upper solid. A uniform normal current passes through all three layers, and the stability of small perturbations to the fluid–fluid interface is analysed. Plane waves are described which can be of either constant or exponentially growing amplitude, depending on the form of the magnetic field due to distant current sources. A model of an electric arc furnace in which the upper layer too is fluid is considered, and in this case MHD effects can also be destabilizing.

1. Introduction

A typical aluminium reduction cell (or (Hall–Héroult cell) carries a current of order 10^5 A. Associated with this current is a strong magnetic field, and one would expect the resulting Lorentz forces to have an important influence on fluid flow in the cell. In essence the cell consists of a layer of molten cryolite (a mixture of sodium and aluminium fluorides) floating on a pool of liquid aluminium. Current is passed into the cell via a block of carbon immersed in the cryolite, and withdrawn via the liquid aluminium (figure 1*a*).

MHD effects can cause difficulties in cell operation (Lympny, Evans & Moreau 1983). In particular, Lorentz forces distort the upper surface of the aluminium pool so that it adopts a curved shape, making it difficult to bring the carbon anode as close as possible to the liquid aluminium and hence reduce the cell resistance and power consumed. Also, instabilities can occur if the cryolite layer is too thin, resulting in contact between the aluminium and the carbon anode, and a dangerous short circuit. It is easy to imagine the sort of mechanism that might drive this instability. The cryolite layer is a poor electrical conductor in comparison with aluminium or carbon, so any perturbation in layer thickness would cause a redistribution of electric current – towards and through the narrowest part of the layer. The consequent changes in magnetic field and Lorentz forces could set up a flow tending to increase the perturbation.

The magnetic field and current distribution in an aluminium reduction cell are complicated (Lympny *et al.* 1983) and the liquid layers are in motion, so to obtain a tractable mathematical problem, some idealization is necessary. In §§2 and 3 we consider a model consisting of a plane horizontal fluid layer of low electrical conductivity and thickness h , sandwiched between two semi-infinite highly conducting layers, the upper one solid (carbon anode) and the lower fluid (liquid aluminium). In the unperturbed state a uniform normal electric current flows through all three layers and there is no fluid motion. The lower fluid layer is taken to be denser than

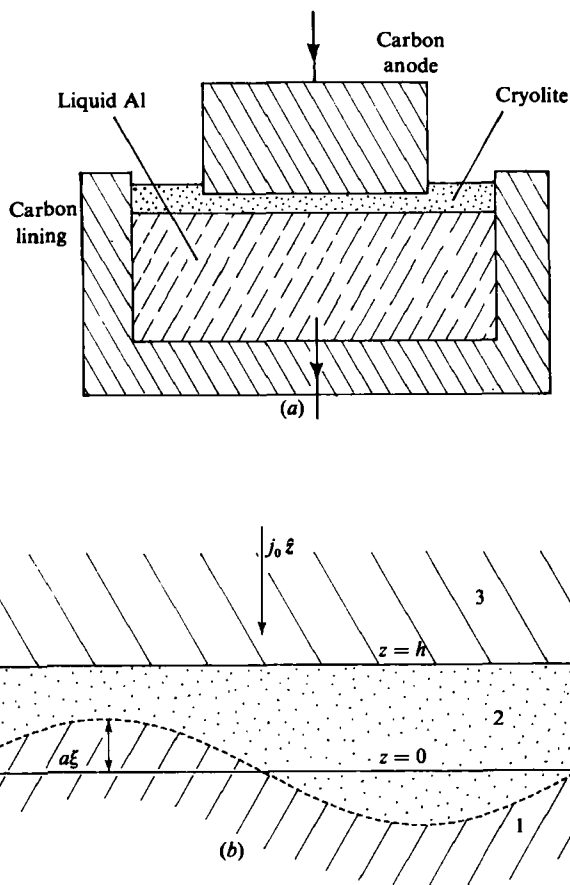


FIGURE 1. (a) Schematic diagram of Hall-Héroult cell. (b) Diagram of the three-layer system.

the middle one, so that the stratification is stable. A linear stability analysis is carried out, assuming that the perturbation growth time is large compared with the magnetic diffusion time over a perturbation wavelength, so that electric current and magnetic fields can be calculated by static methods. The unperturbed magnetic field can be divided into two parts – a local component due to local currents, and a far component due to remote currents. The local component is always stabilizing, reinforcing the gravitational restoring force, and giving rise to waves very similar to surface gravity waves but with a modified dispersion relation to take account of MHD effects. On the other hand the far field can be destabilizing and give rise to waves of exponentially growing amplitude. Since the far field imposes a preferred direction, these waves are anisotropic and the growth rate depends on the direction of the wavenumber vector.

Section 4 considers the problem in which all three layers are fluid – a situation that occurs in an electric-arc furnace, where the upper layer is ionized gas, the middle layer slag, and the lower layer molten metal. The far field can destabilize this system, as in an aluminium cell, but the local field will also be destabilizing if sufficiently strong.

When carrying out a linear stability analysis, one is usually dealing with a homogeneous system, so that it is possible to find plane-wave solutions which can be superposed. A peculiar difficulty of this system is that, since $\nabla \times \mathbf{B} = \mu_0 j_0 \hat{\mathbf{z}}$, the equilibrium magnetic field cannot be homogeneous, but must vary linearly with horizontal position. The Lorentz force perturbation can be expressed, however, as

the sum of a purely horizontal component \mathbf{F}_H and an irrotational component, which can be absorbed into the pressure gradient. The elevation of the cryolite–aluminium interface is governed by the divergence of the horizontal flow, and hence by $\nabla \cdot \mathbf{F}_H$, in which term the linear horizontal spatial dependence disappears. Thus it is possible to find plane waves in which the surface elevation has constant amplitude, while the fluid-flow amplitude varies linearly with horizontal position.

2. Analysis of Lorentz force

Our aim is to carry out a linear stability analysis of the system consisting of three electrically conducting layers of infinite horizontal extent, $-\infty < z < 0$, $0 < z < h$ and $h < z < \infty$, which we call layers 1, 2 and 3 respectively (see figure 1*b*). A variable with a suffix i will be used to denote a value in layer i – for example σ_1 , σ_2 and σ_3 are the electrical conductivities of the three layers. Layers 1 and 2 are fluid (liquid aluminium and cryolite) and layer 3 is solid (the carbon anode). The fluids are assumed incompressible and inviscid, and surface tension is neglected.

Equilibrium

In the equilibrium state a normal current $j_0 \hat{\mathbf{z}}$ passes through all three layers and the fluid–fluid interface $z = 0$ is undisturbed. Since there is no fluid motion, the Lorentz force (which must be balanced by a pressure gradient) is irrotational and

$$\nabla \times (j_0 \hat{\mathbf{z}} \times \mathbf{B}_i) = 0 \quad \text{or} \quad \frac{\partial \mathbf{B}_i}{\partial z} = 0, \quad i = 1, 2. \quad (2.1)$$

The magnetic field must be continuous across any interface, so \mathbf{B} is the same function of (x, y) throughout all layers, and the subscript may be omitted without ambiguity. For the purpose of analysing local stability we assume \mathbf{B} is a linear function of position:

$$\mathbf{B}_i = \mathbf{B}_{0i} + \alpha_{ij} x_j, \quad (2.2)$$

where \mathbf{B}_0 is a constant vector and α_{ij} a constant second-order tensor, which can be expressed as the sum of an antisymmetric part $\alpha_{ij}^{(a)}$ and a symmetric part $\alpha_{ij}^{(s)}$. The rotational field $\alpha_{ij}^{(a)} x_j$ is due to the local current distribution $j_0 \hat{\mathbf{z}}$, and (2.1) combined with Ampère's law

$$\nabla \times \mathbf{B} = \mu_0 j_0 \hat{\mathbf{z}}$$

gives

$$\alpha_{ij}^{(a)} = \begin{bmatrix} 0 & -\frac{1}{2}\mu_0 j_0 & 0 \\ \frac{1}{2}\mu_0 j_0 & 0 & 0 \\ 0 & 0 & 0 \end{bmatrix}. \quad (2.3)$$

The irrotational field $\alpha_{ij}^{(s)} x_j$ is due to remote current sources, such as the bus bars bringing current to the system. Equation (2.1) and the condition that \mathbf{B} be solenoidal show that $\alpha_{ij}^{(s)}$ must be of the form:

$$\alpha_{ij}^{(s)} = \mu_0 j_0 \begin{bmatrix} Q & R & 0 \\ R & -Q & 0 \\ 0 & 0 & 0 \end{bmatrix}, \quad (2.4)$$

where Q and R are constants. Combining (2.3) and (2.4) gives

$$\alpha_{ij} = \mu_0 j_0 \begin{bmatrix} Q & R - \frac{1}{2} & 0 \\ R + \frac{1}{2} & -Q & 0 \\ 0 & 0 & 0 \end{bmatrix}. \quad (2.5)$$

The Lorentz force can be written in the form

$$j_0(\hat{\mathbf{z}} \times \mathbf{B})_i = j_0(\hat{\mathbf{z}} \times \mathbf{B}_0)_i + j_0 \tilde{\alpha}_{ij} x_j, \quad (2.6)$$

where

$$\tilde{\alpha}_{ij} = \mu_0 j_0 \begin{bmatrix} -R^{-\frac{1}{2}} & Q & 0 \\ Q & R^{-\frac{1}{2}} & 0 \\ 0 & 0 & 0 \end{bmatrix}. \quad (2.7)$$

The equilibrium pressure distribution is given by

$$p_i = p_0 - \rho_i g z + p_M(x, y), \quad i = 1, 2,$$

where g is the acceleration due to gravity, and the magnetic component of the pressure

$$p_M = \mu_0 j_0 (\hat{\mathbf{z}} \times \mathbf{B}_0) \cdot \mathbf{x} + \mu_0 j_0^2 [Qxy - \frac{1}{4}(x^2 + y^2) + \frac{1}{2}R(y^2 - x^2)].$$

Current perturbation

Suppose that the interface $z = 0$ suffers a small perturbation, so that its equation becomes

$$z = a\xi(x, y, t) = a e^{\omega t} f(x, y),$$

where a ($\ll h$) is a constant amplitude, ω a (complex) growth rate and f is such that $f \exp(\pm kz)$ is harmonic. For example one could take

$$f = \exp[i(lx + my)], \quad l^2 + m^2 = k^2, \quad (2.8)$$

to represent a plane-wave disturbance, or

$$f = J_0(kr), \quad r^2 = x^2 + y^2, \quad (2.9)$$

for a disturbance symmetric about the z -axis.

If we suppose that the disturbance growth time ω^{-1} is large compared with the magnetic diffusion time $k^{-2}\mu_0\sigma$, the electric and magnetic fields will be approximately static, so that

$$\nabla \times \mathbf{E} = 0.$$

The usual MHD approximation of neglecting displacement current is also made, so that the electric current density \mathbf{j} satisfies

$$\nabla \cdot \mathbf{j} = 0, \quad \mathbf{j} = \sigma \mathbf{E} \quad (\text{Ohm's law}).$$

It follows that the current in the three layers can be expressed in the form

$$\mathbf{j}_i = j_0 \hat{\mathbf{z}} + \mathbf{j}'_i = j_0(\hat{\mathbf{z}} + \nabla \phi_i),$$

where the functions ϕ_i must be harmonic, so that we can write

$$\phi_1 = \alpha_1 \xi e^{kz}, \quad (2.10)$$

$$\phi_2 = \xi(\alpha_2 e^{kz} + \beta_2 e^{-kz}) = \phi_2^+ + \phi_2^- \text{ say,} \quad (2.11)$$

$$\phi_3 = \beta_3 \xi e^{-kz}. \quad (2.12)$$

The constant coefficients α_i , β_i are determined from the four equations expressing continuity of normal current and tangential electric field across the interfaces $z = 0$, $z = h$:

$$\alpha_1 = \frac{a(1-r_2)(r_2s+r_3c)}{(r_2+r_3r_2)c+(r_3+r_2^2)s}, \quad (2.13)$$

$$\alpha_2 = \frac{ae^{-kh}(r_3-r_2)(1-r_2)}{2c(r_2+r_3r_2)+2s(r_3+r_2^2)}, \quad (2.14)$$

$$\beta_2 = \frac{-ae^{kh}(r_3+r_2)(1-r_2)}{2c(r_2+r_3r_2)+2s(r_3+r_2^2)}, \quad (2.15)$$

where $r_2 = \sigma_2/\sigma_1$, $r_3 = \sigma_3/\sigma_1$, and $s = \sinh kh$, $c = \cosh kh$. (The formula for β_3 is not given since it will not be needed.) Of particular interest is the case when the middle layer has a much lower electrical conductivity than the other two - i.e. when $r_2 \ll 1$. Then (2.13)–(2.15) simplify to

$$\alpha_1 = \frac{ac}{s}, \quad \alpha_2 = \frac{ae^{-kh}}{2s}, \quad \beta_2 = \frac{-ae^{kh}}{2s}. \quad (2.16)$$

The perturbation magnetic fields due to the current perturbations, are denoted by B'_i and it is easily verified that the following expressions satisfy Ampère's law, $\nabla \times B'_i = \mu_0 j_0 \nabla \phi_i$:

$$B'_1 = \frac{\mu_0 j_0}{k} \nabla \phi_1 \times \hat{z}, \quad (2.17)$$

$$B'_2 = \frac{\mu_0 j_0}{k} (\nabla \phi_2^+ - \nabla \phi_2^-) \times \hat{z}, \quad (2.18)$$

$$B'_3 = -\frac{\mu_0 j_0}{k} \nabla \phi_3 \times \hat{z}. \quad (2.19)$$

Continuity of tangential magnetic field across either interface follows from continuity of normal current, and the vertical component of B is unaffected by the perturbation, so the above expressions satisfy all necessary equations.

Body force

The Lorentz force perturbation F is given by

$$F = j' \times B + j_0 \hat{z} \times B'.$$

For the stability analysis in the following sections we need to know the divergence of F , and standard vector identities give

$$\nabla \cdot F = -2\mu_0 j_0 j'_z. \quad (2.20)$$

For example

$$\nabla \cdot F_2 = -2\mu_0 j_0^2 k(\phi_2^+ - \phi_2^-).$$

We can also write

$$F = F_H - \frac{1}{\mu_0} \nabla (B \cdot B'). \quad (2.21)$$

where

$$F_H = \frac{1}{\mu_0} (B \cdot \nabla) B' + \frac{1}{\mu_0} (B' \cdot \nabla) B \quad (2.22)$$

is a purely horizontal vector (i.e. has no z -component). Now

$$\begin{aligned} \frac{1}{\mu_0} \nabla^2 (\mathbf{B} \cdot \mathbf{B}'_1) &= \frac{j_0}{k} \nabla^2 [\mathbf{B} \cdot (\nabla \phi_1 \times \hat{\mathbf{z}})] = \frac{j_0}{k} \nabla^2 [\nabla \phi_1 \cdot (\hat{\mathbf{z}} \times \mathbf{B})] \\ &= \frac{2j_0}{k} \frac{\partial^2 \phi_1}{\partial x_\mu \partial x_\nu} [\nabla (\hat{\mathbf{z}} \times \mathbf{B})]_{\mu\nu} \end{aligned} \quad (2.23)$$

(the summation convention applying to μ and ν) since

$$\nabla^2 (\hat{\mathbf{z}} \times \mathbf{B}) = \nabla^2 (\nabla \phi_1) = 0.$$

Equations (2.6), (2.20), (2.21) and (2.23) combine to give

$$\nabla \cdot \mathbf{F}_{H1} = -2\mu_0 j_0^2 k \phi_1 + \frac{2j_0}{k} \frac{\partial^2 \phi_1}{\partial x_\mu \partial x_\nu} \tilde{\alpha}_{\mu\nu}, \quad (2.24)$$

and a similar equation holds for $\nabla \cdot \mathbf{F}_{H2}$. In particular, for plane waves when the disturbance function f is given by (2.8) we find

$$\nabla \cdot \mathbf{F}_{H1} = \frac{2b\phi_1}{k}, \quad \nabla \cdot \mathbf{F}_{H2} = \frac{2b(\phi_2^+ - \phi_2^-)}{k}, \quad (2.25)$$

where

$$b = \mu_0 j_0^2 [R(l^2 - m^2) - 2Qlm - \frac{1}{2}k^2]. \quad (2.26)$$

The first two terms in the square bracket arise from the far magnetic field and the third term from the local field. For axisymmetric waves with f given by (2.9), equations (2.25) and (2.26) remain valid provided we assume that the field due to remote current sources is zero, so that $Q = R = 0$.

3. Dispersion relations

The linearized equation of motion in the fluid layers is

$$\rho \frac{\partial \mathbf{u}}{\partial t} = -\nabla p' + \mathbf{F},$$

where ρ is density, \mathbf{u} the perturbation velocity and p' the pressure perturbation (the viscous term having been neglected). Since the forcing term \mathbf{F} is proportional to $e^{\omega t}$ we expect \mathbf{u} to exhibit the same time dependence, and employing (2.21) we find

$$\rho \omega \mathbf{u} = \mathbf{F}_H - \nabla P, \quad (3.1)$$

where

$$P = p' + \frac{1}{\mu_0} \mathbf{B} \cdot \mathbf{B}'.$$

We assume the fluid to be incompressible, so that $\nabla \cdot \mathbf{u} = 0$ and

$$\nabla^2 P = \nabla \cdot \mathbf{F}_H. \quad (3.2)$$

Equation (3.1) provides formulae for $\mathbf{u}_1, \mathbf{u}_2$, but in terms of the unknown functions P_1, P_2 . The latter can be found by solving (3.2) subject to the boundary conditions obtained from the continuity of u_z and p across the fluid-fluid interface $z = 0$, and

the condition that u_z must vanish at the solid interface $z = h$. To summarize, we must solve

$$\nabla^2 P_1 = \frac{2b}{k} \phi_1, \quad (3.3)$$

$$\nabla^2 P_2 = \frac{2b}{k} (\phi_2^+ - \phi_2^-), \quad (3.4)$$

$$\frac{1}{\rho_1} \left(\frac{\partial P_1}{\partial z} \right)_{z=0} = \frac{1}{\rho_2} \left(\frac{\partial P_2}{\partial z} \right)_{z=0}, \quad (3.5)$$

$$(P_2)_{z=0} - (P_1)_{z=0} = -\Delta\rho g a \xi, \quad \Delta\rho = \rho_1 - \rho_2, \quad (3.6)$$

$$\left(\frac{\partial P_2}{\partial z} \right)_{z=h} = 0. \quad (3.7)$$

The first two equations are derived by combining (3.2) and (2.25). Obvious particular integrals of (3.3) and (3.4) are

$$P_1 = \frac{bz}{k^2} \phi_1, \quad P_2 = \frac{bz}{k^2} (\phi_2^+ + \phi_2^-),$$

so we try general solutions

$$P_1 = \frac{bz}{k^2} \phi_1 + A\phi_1, \quad P_2 = \frac{bz}{k^2} (\phi_2^+ + \phi_2^-) + B\phi_2^+ + C\phi_2^-, \quad (3.8)$$

where A , B and C are arbitrary constants to be determined from the three linear simultaneous equations (3.5)–(3.7). In particular, when layer 2 is weakly conducting, we can use (2.16) and find

$$A = \frac{\Delta\rho g s^2}{\rho c^2 + sc} - bk^{-3} \left(1 + \frac{kh}{s + \rho c} \right), \quad (3.9)$$

where $\rho = \rho_2/\rho_1$.

The dispersion relation is obtained from the kinematic boundary condition on the fluid–fluid interface:

$$a\omega\xi = (u_z)_{z=0} = -\frac{1}{\rho_1\omega} \left(\frac{\partial P_1}{\partial z} \right)_{z=0} = -\frac{1}{\rho_1\omega} \left(\frac{b}{k^2} + kA \right) (\phi_1)_{z=0},$$

or

$$\omega^2 = -\frac{\alpha_1}{a\rho_1} \left(\frac{b}{k^2} + kA \right). \quad (3.10)$$

For simplicity we consider only the case of a weakly conducting layer 2, when we can substitute (3.9) into (3.10) to find

$$\omega^2 = \frac{(bch/k) - \Delta\rho gks^2}{\rho_2 cs + \rho_1 s^2}. \quad (3.11)$$

When $j_0 = 0$ and there are no MHD effects, (3.11) reduces to the gravity-wave dispersion relation. A positive value of ω^2 corresponds to instability, so the effect of the currents is stabilizing if $b < 0$ and destabilizing if $b > 0$. From (2.26) we see that the term $-\frac{1}{2}k^2$, which arises from the local rotational magnetic field, is always stabilizing. If $Q = R = 0$

$$\omega = \pm i \left[\frac{\frac{1}{2}\mu_0 j_0^2 khc + \Delta\rho gks^2}{\rho_2 cs + \rho_1 s^2} \right]^{\frac{1}{2}},$$

for plane waves with wavevector $\mathbf{k} = (l, m, 0)$. The corresponding formula for axisymmetric waves is identical.

On the other hand, the effect of the far field can be destabilizing. Since

$$R(l^2 - m^2) - 2Qlm = -k_i \alpha_{ij}^{(s)} k^j, \quad (3.11)$$

where $\mathbf{k}^p = \mathbf{k} \times \hat{\mathbf{z}}$, the expression on the left-hand side is invariant and can be most conveniently evaluated in the principal axes $OX'Y'$ of the tensor $\alpha_{ij}^{(s)}$. The eigenvalues are $\pm(Q^2 + R^2)^{1/2} = \pm\alpha$, say, and we suppose that the x' direction corresponds to the positive eigenvalue. One finds that

$$b = \mu_0 j_0^2 k^2 (\alpha \sin 2\chi - \frac{1}{2}), \quad (3.12)$$

where χ is the angle between the x' axis and \mathbf{k} . The fastest-growing instability occurs when $\chi = \frac{1}{4}\pi$.

Group velocity of stable waves

When the system is stable, the dispersion relation for plane-wave disturbances proportional to $\exp[i(\mathbf{k} \cdot \mathbf{x} - \Omega t)]$ can be found by combining (3.11) and (3.12):

$$\Omega^2 = \frac{\Delta\rho gks^2 + \frac{1}{2}\mu_0 j_0^2 kch(1 - 2\alpha \sin 2\chi)}{\rho_2 cs + \rho_1 s^2}.$$

When $\alpha = 0$, Ω^2 depends on only the magnitude of \mathbf{k} and the dispersion is isotropic, the group velocity being parallel to and smaller in magnitude than the phase velocity, as for gravity waves. When $\alpha > 0$ the far field imposes a preferred direction. This anisotropy is most extreme when $\rho_1 = \rho_2$, $kh \ll 1$ and

$$\Omega^2 \approx \frac{\mu_0 j_0^2}{\rho_1} (\frac{1}{2} - \alpha \sin 2\chi) = \frac{\mu_0 j_0^2}{\rho_1} \left(\frac{1}{2} - \frac{2\alpha l' m'}{k^2} \right), \quad (3.13)$$

where l' , m' are the components of \mathbf{k} relative to the principal axes of $\alpha_{ij}^{(s)}$. Now Ω depends on only the direction of \mathbf{k} and the group velocity

$$\mathbf{c}_g = \frac{\alpha \mu_0 j_0^2}{\rho_1 k^4 \Omega} (m'^2 - l'^2) (-m', l')$$

is perpendicular to \mathbf{k} so that energy is propagated along the wave crests. If $\alpha = 0$, so that the only force tending to restore layer disturbances is that due to the local magnetic field, then $\mathbf{c}_g = 0$ and a local disturbance will not propagate. Generally \mathbf{c}_g will have components both parallel and perpendicular to \mathbf{k} .

Flow field

In order to visualize the fluid flow associated with these plane waves we consider a simple case with no far magnetic field ($Q = R = 0$), and also eliminate the effect of density differences by setting $\rho_1 = \rho_2$. For these waves ω is purely imaginary $= -i\Omega$, say. Using (2.2), (2.3), (2.10), (2.16), (2.22), (3.1), (3.8) and (3.9), we find

$$\begin{aligned} \frac{2\rho_1 \Omega}{\alpha_1 \mu_0 j_0^2} \mathbf{u}_1 = & e^{kz} k(h' - z) \cos(kx - \Omega t) \hat{\mathbf{x}} \\ & + e^{kz} ky \sin(kx - \Omega t) \hat{\mathbf{y}} + e^{kz} k(h' - z) \sin(kx - \Omega t) \hat{\mathbf{z}}, \end{aligned} \quad (3.14)$$

where the constant $h' = h e^{-kh}$, and the x -axis has been chosen parallel to \mathbf{k} . (By a suitable choice of origin, the constant term \mathbf{B}_0 in the magnetic-field expansion (2.1), can be taken to be zero.) The streamlines for the flow at $t = 0$ have equations

$$x = k^{-1} \cos^{-1}(K_1 e^{-kz}), \quad y = \frac{K_2}{k(z-h')}, \quad (3.15a, b)$$

where K_1, K_2 are arbitrary constants. The families of curves given by (3.15) are sketched in figure 2. Streamlines beginning on the plane $y = 0$ remain on that plane, while those beginning from points where y is non-zero lie on the hyperbolic surface whose equation is (3.15b).

Assuming that the amplitude a is small enough so that the fluid particles deviate only slightly from their mean positions, we can also use (3.14) to find the fluid-particle paths. If (x_P, y_P, z_P) denotes the position of a fluid particle whose mean position is (x, y, z) then

$$x_P = x - a' e^{kz} k(h' - z) \sin(kx - \Omega t),$$

$$y_P = y + a' e^{kz} ky \cos(kx - \Omega t),$$

$$z_P = z + a' e^{kz} k(h' - z) \cos(kx - \Omega t),$$

where $a' = \alpha_1 \mu_0 j_0^2 / 2\rho_1 \Omega^2$. Fluid particles in the plane $y = 0$ move in circles whose radii decrease with depth (just as in surface gravity waves). Particles not on $y = 0$ move in elliptical paths, which lie in planes inclined at an angle $\tan^{-1}[y/(h' - z)]$ to $y = 0$. These paths are sketched in figure 3.

4. Three fluid layers

The problem in which layer 3 is a fluid is also of interest, since this is a model of the electric-arc furnace. Now there are two fluid-fluid interfaces, $z = 0$ and $z = h$, and for a plane-wave disturbance the perturbed surface equations will be

$$z = \eta_1 = a_1 \exp[i(lx + my) + \omega t], \quad (4.1)$$

$$z = h + \eta_2 = h + a_2 \exp[i(lx + my) + \omega t], \quad (4.2)$$

where a_1 and a_2 are (small) complex amplitudes. The corresponding electric-current perturbations are given as before by (2.10)–(2.12), and the unknown coefficients $\alpha_1, \alpha_2, \beta_2, \beta_3$ are found by solving the four simultaneous equations expressing continuity of normal current and tangential electric field across the two interfaces. When layer 2 is weakly conducting ($r_2 \ll 1$) the solutions are

$$\alpha_1 = \frac{a_1 c - a_2}{s}, \quad \alpha_2 = \frac{a_1 e^{-kh} - a_2}{2s}, \quad \beta_2 = \frac{a_2 - a_1 e^{kh}}{2s}. \quad (4.3)$$

The corresponding magnetic-field perturbations are given by (2.17)–(2.19). As before, we divide the Lorentz-force perturbation \mathbf{F} into a horizontal component and an irrotational component, so that the linearized equations of fluid motion are

$$\rho_i \omega \mathbf{u}_i = \mathbf{F}_{Hi} - \nabla P_i, \quad i = 1, 2, 3.$$

The functions P_i must satisfy the Poisson equations

$$\nabla^2 P_1 = \frac{2b}{k^2} \phi_1, \quad \nabla^2 P_2 = \frac{2b}{k^2} (\phi_2^+ - \phi_2^-), \quad \nabla^2 P_3 = \frac{-2b}{k^2} \phi_3,$$

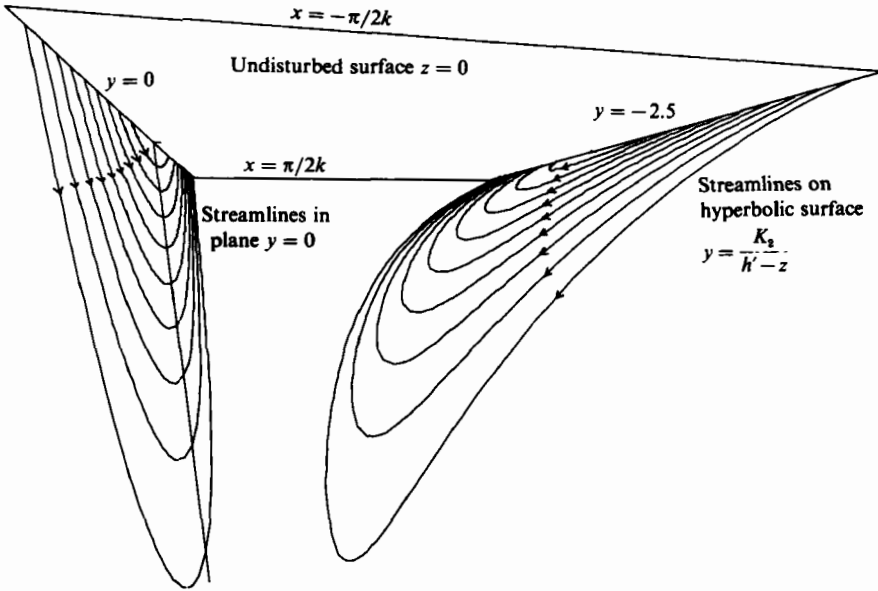


FIGURE 2. Streamlines in layer 1 viewed from $(-3, -1, -3)$, when the far field is zero and the wavenumber vector in the direction of the positive x -axis.

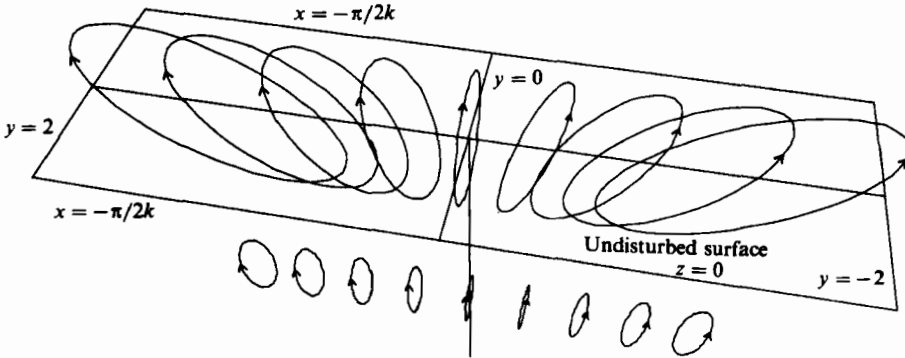


FIGURE 3. Particle paths in layer 1 viewed from $(-5, -3, 5)$, when the far field is zero and the wavenumber vector in the direction of the positive x -axis. In the plane $y = 0$ the paths are circles. Elsewhere they are tilted ellipses.

which have general solutions

$$P_1 = \frac{bz}{k} \phi_1 + A\phi_1, \quad P_2 = \frac{bz}{k} (\phi_2^+ + \phi_2^-) + B\phi_2^+ + C\phi_2^-, \quad P_3 = \frac{bz}{k} \phi_3 + D\phi_3,$$

where A, B, C and D are arbitrary constants. The continuity of normal velocity and pressure across the two interfaces together with the two kinematic boundary conditions ($u_z = \partial\eta/\partial t$) provide a linear homogeneous system of six equations in the six variables $A\alpha_1, B\alpha_2, C\beta_2, D\beta_3, a_1$ and a_2 . The condition that the coefficient determinant vanish yields the dispersion relation. Since we are modelling an arc furnace, in which the upper layer (layer 3) is an ionized gas, a reasonable simplification

is to set $\rho_3 = 0$. We also assume $\rho_2 < \rho_1$ (slag density < liquid-steel density) so that the stratification is stable. The dispersion relation obtained is

$$\omega^4 \rho_2 (c\rho_1 + s\rho_2) + \omega^2 \left[\rho_1 \rho_2 gk(s+c) - \frac{\rho_1 bh}{ks} \right] + gk \left(\rho_2 \Delta \rho gks - \frac{bh}{ks} \right) - \frac{b^2 h^2}{k^2 s^2} = 0. \quad (4.4)$$

Equation (4.4) can be written in non-dimensional form as

$$\omega'^4 \rho(c + s\rho) + \omega'^2 [\rho(s+c) - Js^{-1}] + \rho(1-\rho)s - Js^{-1} - J^2 s^{-1} = 0, \quad (4.5)$$

where

$$\omega'^2 = \frac{\omega^2}{gk}, \quad \rho = \frac{\rho_2}{\rho_1},$$

and

$$J = \frac{bh}{\rho_1 gk^2} = \frac{\mu_0 j_0^2 h}{\rho_1 g} \left(\alpha \sin 2\chi - \frac{1}{2} \right)$$

is a dimensionless measure of the current strength.

Equation (4.5) is a quadratic in ω'^2 , and it can be shown by simple algebra that the discriminant is positive, so that the roots are always real. Positive roots correspond to unstable disturbances and negative roots to neutrally stable or wavelike ones. Since the coefficient of ω'^4 is positive there will always be a positive root if the constant term is negative. There might also be a positive root if the constant term were positive and the coefficient of ω'^2 negative, but some simple algebra can eliminate this possibility. Thus the condition for stability is:

$$J^2 + J - \rho(1-\rho)s^2 < 0,$$

or

$$J_1 < J < J_2, \quad (4.6)$$

where $J_1 = -\frac{1}{2}\{[1+4s^2\rho(1-\rho)]^{\frac{1}{2}}+1\}$, $J_2 = \frac{1}{2}\{[1+4s^2\rho(1-\rho)]^{\frac{1}{2}}-1\}$.

A particularly simple case occurs when the density ratio $\rho = \frac{1}{2}$, and $J_1 = -\frac{1}{2}(c+1)$, $J_2 = \frac{1}{2}(c-1)$. Figure 4 shows graphs of J_1 and J_2 against dimensionless wavenumber kh , indicating the stable and unstable regions. MHD effects are most destabilizing for long wavelengths ($kh \ll 1$), when $J_1 = -1$ and $J_2 = 0$. For very short wavelengths MHD effects are negligible, and the density stratification provides stability. It is interesting that the stability depends on the density ratio ρ in a symmetric way, and that gravity exerts the greatest stabilizing influence when $\rho = \frac{1}{2}$. If $\rho = 1$ or 0 this stabilizing influence will be absent from the lower or upper interface respectively, and the stability condition is just $-1 < J < 0$ - independent of wavelength.

If (3.11) is also non-dimensionalized the stability condition for the aluminium cell model (layer 3 rigid) becomes

$$J < (1-\rho)s^2/c, \quad (4.7)$$

which is similar in form to the stability condition (4.6) for positive J , namely

$$J < \frac{1}{2}\{[1+4s^2\rho(1-\rho)]^{\frac{1}{2}}-1\}. \quad (4.8)$$

When the far magnetic field gives rise to a positive b , and hence positive J , then in both cases instability can occur for any given wavenumber, provided the layer depth h is small enough. Since J is proportional to h , maintaining k fixed and decreasing h corresponds to moving inward along the line L in figure 4, from a stable region to an unstable one, and eventually violating (4.8). A similar argument holds for (4.7). The novel feature of the arc furnace or all-fluid problem is that instability is also possible for $J < -1$, so that local currents can be destabilizing if sufficiently strong - if $\mu_0 j_0^2 > 2\rho_1 g/h$ for example, in the case of zero far field.

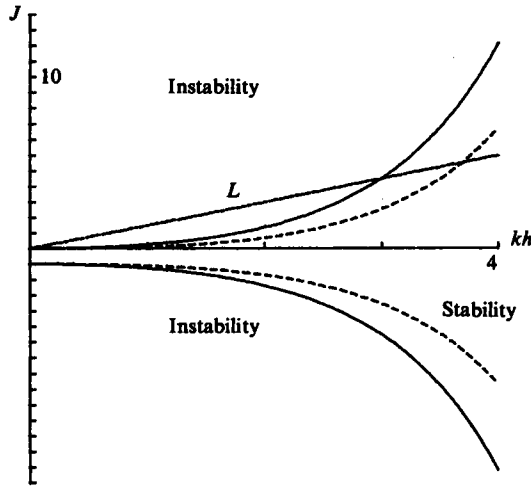


FIGURE 4. Stability of the three-fluid-layer system. The solid curves correspond to $\rho = \frac{1}{2}$, which is the widest stability region, and the dashed curves to $\rho = 0.1$ or 0.9 .

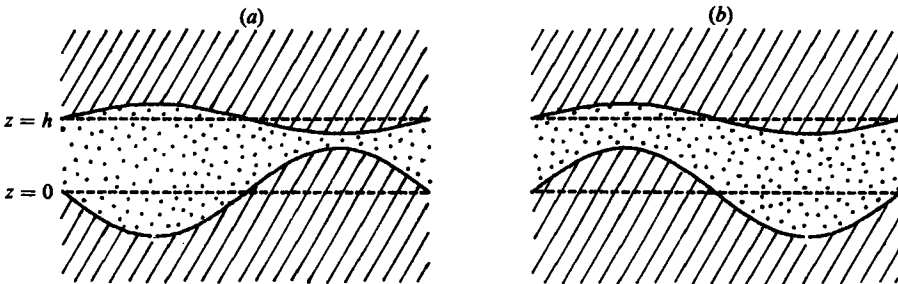


FIGURE 5. Forms of unstable disturbances to the three-fluid-layer system. In (a) $J > 0$ and the disturbance is of the sausage type, and in (b) $J < -1$ and it is of the kink type.

The calculations involved in finding the dispersion relation also show that

$$\frac{a_1}{a_2} = \frac{-(J + \rho)}{\omega'^2(c + s\rho) + c(1 - \rho)}.$$

Thus positive- J instabilities are of the 'sausage' type - a_1 and a_2 having opposite signs - whereas the negative- J instabilities are of the 'kink' type, since $J < -1$ (see figure 5).

5. Discussion

The dispersion relation (3.11) shows that the criterion for instability is

$$bch/k > \Delta\rho gks^2.$$

We can write $b = b'\mu_0 J_0^2 k^2$, where b' is a dimensionless number of order unity, and the condition then becomes

$$\frac{h \cosh kh}{\sinh^2 kh} > \frac{\Delta\rho g}{b'\mu_0 J_0^2}. \tag{5.1}$$

Inserting typical values (in SI units) $\Delta\rho = 10^3$, $g = 10$, $\mu_0 = 4\pi \times 10^{-7}$ and $j_0 = 2 \times 10^4$, (5.1) gives

$$\frac{h \cosh kh}{\sinh^2 kh} > \frac{20}{b'} \quad (5.2)$$

as the instability condition. The cryolite-layer depth h is typically of order 4×10^{-2} m, so if kh is large the left-hand side of (5.2) will be small. Thus, small-wavelength disturbances will be stable. On the other hand, if kh is small the left-hand side will be approximately $(k^2h)^{-1}$, so instability is possible for long wavelengths, say of order 1 m, which is still somewhat less than the dimension of a typical cell – namely 3×8 m. It can be seen that the neglect of surface tension is justified, since we are most interested in longer wavelengths, where MHD effects are important.

Since the left-hand side of (5.2) tends to infinity as $h \rightarrow 0$, instability is always possible for a narrow-enough cryolite layer. The reason is that the stabilizing buoyancy force is proportional to the absolute magnitude a of the surface displacement, but changes in current and magnetic field (caused by the tendency of the current to flow through the narrow part of the layer) will vary as the relative change in layer resistance – i.e. as a/h . Thus for small h MHD forces will dominate.

Wave damping due to viscosity has also been neglected. Equation (73) of Lighthill (1978) shows that in the long-wavelength limit the damping factor (or proportional loss of amplitude over each wave period) due to energy dissipation in the viscous boundary layer adjacent to the rigid surface is

$$\frac{\pi}{h} \left(\frac{\nu}{\omega} \right)^{\frac{1}{2}},$$

where ν is the cryolite viscosity. Unless MHD effects completely overwhelm gravity, we can set $\omega \approx k(gh)^{\frac{1}{2}}$, so, if $h = 4 \times 10^{-2}$ and the wavelength 1 m, the damping factor is $39.6\nu^{\frac{1}{2}}$. The value of ν is uncertain since the flow in the cryolite layer is turbulent, and some sort of eddy viscosity might be appropriate – in which case viscous damping could be a significant stabilizing influence.

We have also neglected changes in the buoyancy force due to thermal effects. If Δj_0 represents a typical change in the current density, then the change ΔF in the Lorentz force is given by

$$\Delta F = \mu_0 j_0 \Delta j_0 L,$$

where L is wavelength. The change in buoyancy force due to the local change in ohmic heating over a wave period is given by

$$g \Delta\rho = \rho g \frac{j_0 \Delta j_0 \alpha_E}{\sigma \omega c_s},$$

where α_E is the volume expansion coefficient and c_s the specific heat per unit volume of the cryolite. (Heat diffusion, which will tend to smooth out local temperature changes, has been neglected, so we are overestimating thermal effects.) Thus

$$\frac{g \Delta\rho}{\Delta F} = \frac{\rho g \alpha_E}{\omega \mu_0 \sigma L c_s} = O(10^{-1}),$$

so thermal effects will be less important than MHD effects.

It is now possible to examine the validity of the magnetostatic approximation

$$\omega^{-1} \gg k^{-2} \mu_0 \sigma \quad (5.3)$$

made when calculating the perturbation electric current and magnetic fields. Assuming that MHD effects are at least as important as buoyancy (which is the situation of interest), it then follows from (3.11) and (2.21) that

$$\omega^2 \approx \frac{\mu_0 j_0^2 khc/s}{\rho_2 c + \rho_1 s}.$$

If we assume kh is small and substitute typical values for j_0 , ρ_2 , and σ (we use the value for liquid aluminium, since this has the highest conductivity and is therefore the layer through which the magnetic field diffuses most slowly) then (5.3) reduces to the condition:

$$k^2 > 8.8 \text{ m}^{-2}.$$

This condition will be satisfied for wavelengths less than about 1 m (when $k = 2\pi \text{ m}^{-1}$), which is the area of interest.

The most-unrealistic assumptions made in this analysis are probably that of a uniform normal current, and no fluid motion in the unperturbed state. Also we have neglected the effects of lateral boundaries. The linear spatial variation in the amplitude of u (see e.g. (3.14)) means that reflection of a wavenumber k from a lateral boundary would excite the whole spectrum of possible wavenumbers. To discuss the stability of a bounded system, all wavenumbers would have to be considered simultaneously.

Finally, it is interesting that the stability of the system depends on the form of the magnetic field due to far current sources (see (3.11) and (3.12)). Lympany *et al.* (1983) found that the way in which the current is delivered and withdrawn from the cell has an important influence on the shape of the liquid aluminium surface, and it appears that the geometry of these connections may also influence the stability of that surface shape. Without performing extensive numerical magnetic-field calculations, it would be difficult say exactly how the design of the Hall-Héroult cell should be modified to minimize MHD instabilities. Roughly speaking, the cell should be made as symmetrical as possible to eliminate horizontal gradients in the far field. For a circular cell, with current fed in and withdrawn by a axisymmetric system of conductors, the far-field gradient would be zero at least at the centre, but could not be eliminated near the edges.

I am indebted to a referee for suggesting the method of resolving the magnetic field into local and far components.

REFERENCES

- LIGHTHILL, M. J. 1978 *Waves in Fluids*. Cambridge University Press.
 LYMPANY, S. D., EVANS, J. W. & MOREAU, R. 1983 Magnetohydrodynamic effects in aluminium reduction cells. In *Proc. IUTAM Symp. on Metallurgical Applications of Magnetohydrodynamics, Cambridge, 1982*, pp. 15–23. The Metals Society, London.